

Magnetic-domain structure of $\text{Ni}_{1-x}\text{Mn}_x$ films inferred from resistance fluctuations

C. D. Keener and M. B. Weissman

Department of Physics, University of Illinois at Urbana-Champaign, 1110 West Green Street, Urbana, Illinois 61801

(Received 1 June 1993; revised manuscript received 12 August 1993)

In films of partially ordered $\text{Ni}_{1-x}\text{Mn}_x$ with $x \approx 0.28$, large electrical-resistance noise from magnetic effects was found. Individual fluctuating domains with large volumes but low magnetic moments were observed. These domains are apparently clusters of constituent ferromagnetic domains which have a net systematic antiferromagnetic alignment. The clusters are larger in the "reentrant spin-glass" regime than in the ferromagnetic regime. Ferromagnetic domains arranged in antiferromagnetic stripes were also imaged by scanning electron microscopy.

INTRODUCTION

Fully disordered $\text{Ni}_{1-x}\text{Mn}_x$ has both a ferromagnetic regime and a regime with large magnetic remanence effects, called a reentrant spin glass,¹⁻⁹ similar to a number of other partially random magnetic systems. (See Ref. 10 for reviews.) Figure 1 shows a simple phase diagram.¹¹ While there is unambiguous evidence that ferromagnetic domains persist in the reentrant regime,^{1,2} the nature of the magnetic order among and within those domains remains unclear. Indirect evidence has led to the hypothesis that in the reentrant regime³ clusters of ferromagnetic domains are antiferromagnetically aligned with each other with 180° domain boundaries.⁴

In the high-susceptibility regime above the apparent reentrant temperature, the presence of true ferromagnetic order in material with short-range chemical order, such as slowly quenched bulk samples, has been questioned.¹² The evidence against long-range magnetic order is the lack of critical behavior near the onset of the high-susceptibility regime.¹² Since critical behavior is obscured by inhomogeneity, and bulk thermal quenching is intrinsically inhomogeneous, probes of long-range order *within* the high-susceptibility regime are desirable. The main purpose of this paper is to demonstrate that equilibrium fluctuations can reveal striking qualitative properties of the magnetic order and dynamics even in such imperfect samples.

In this paper we report the presence of substantial electrical-resistance noise from magnetic effects in $\text{Ni}_{1-x}\text{Mn}_x$ films. In the high-susceptibility, ferromagnetic-like regime we find large coherently switching domain clusters, with small net magnetic moments. In the reentrant regime we find even larger individual switching events with smaller associated moments. Also, via scanning electron microscopy (SEM) we directly observed ferromagnetic domains arranged antiferromagnetically. Our results point directly to the existence of domain clusters of the type postulated by Kouvel and Abdul-Razzaq³ for the reentrant regime.

BACKGROUND

Ferromagnetic $\text{Ni}_{1-x}\text{Mn}_x$ has a large spontaneous resistive anisotropy (SRA),¹³ meaning that the resistivity

(ρ) parallel to the magnetization within a ferromagnetic domain differs significantly from ρ perpendicular to the magnetization. Thus the resistance R , measured along any particular current direction, is sensitive to rotations of domains by any angles other than 180° . Since magnetization itself is most sensitive to rotations of 180° , resistance and magnetization measurements obviously provide somewhat different information.

The presence of "wasp-waisted" zero-field-cooled magnetic hysteresis loops, together with the absence of large accompanying resistance hysteresis effects,⁵ provides the best evidence for the special role of 180° domain walls in the reentrant regime.³⁻⁵ This unusual hysteresis is believed to result from the bimodal distribution of exchange fields seen by the different domains.

We shall see that the magnetic characterization of our film samples indicates significant differences from the most rapidly quenched bulk disordered samples.¹² The magnetic behavior of our samples most closely resembles those of bulk samples in which some atomic short-range order is present.^{12,14} In such bulk samples inhomogeneities often make it impossible to infer the nature of the magnetic order from critical behavior. Thus the ex-

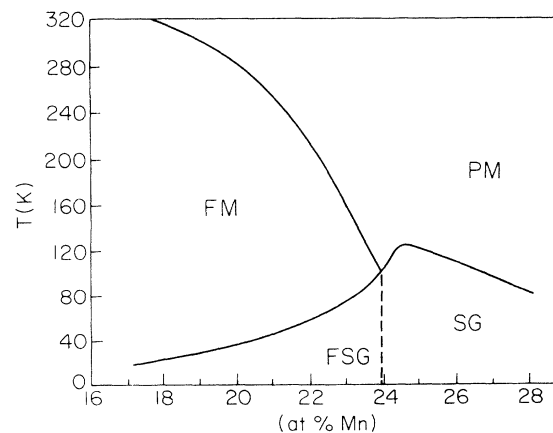


FIG. 1. Phase diagram of bulk disordered $\text{Ni}_{1-x}\text{Mn}_x$, after Ref. 11. PM refers to the paramagnetic phase, FM to ferromagnetic, SG to the pure spin glass, and FSG to the mixed ferro-spin-glass phase.

tent of any ferromagnetic order in such samples has not previously been determined.¹² Here we will present SEM images which confirm that small ferromagnetic domains cover at least something on the order of half of the sample surface. Contrast between alternate domains was insufficient to be certain about the remainder of the film. The size of the domain clusters inferred from the noise will indicate that long-range magnetic order is in fact present in our samples.

We shall be concerned especially with a type of domain reorientation to which the resistance is disproportionately sensitive and the magnetization relatively insensitive. We will show that this type of domain reorientation must involve dynamically coherent clusters of domains. Experimentally, Barkhausen noise is found to vanish as the reentrant regime is approached from the ferromagnetic regime,¹¹ indicating that, at least at low fields, no domains which have a large net ferromagnetic moment are free to reorient. However, in the resistance we observe spontaneous reorientations of individual, large, regions with coherent resistive anisotropy but with small magnetic moments.

We shall show that the large size of the resistance steps, together with the known SRA of domains, sets a minimum volume for the rotating, magnetically ordered regions. However, their surprisingly small sensitivity to magnetic fields sets a maximum net magnetic moment per such region. Together, these effects lead to the 180° domain-cluster model which has been proposed for the reentrant regime,³ except that in our films such clustering, along with significant remanence, extends well into the ferromagnetic regime.

A number of parameters need to be defined before we can proceed further. Also, some of the simple calculations to be used in the rest of the paper are performed here in order to streamline the discussion of our results.

The large SRA in Ni_{1-x}Mn_x (Ref. 13) couples the magnetic domain fluctuations to the resistance. When a domain switches between two different orientations, the fractional step size in the resistance $\Delta R/R$ due to the SRA is

$$\frac{\Delta R}{R} = \frac{\Delta\rho}{\rho} \frac{V_D}{V_s} (\cos^2\theta_1 - \cos^2\theta_2), \quad (1)$$

where $\Delta\rho/\rho$ is the SRA, θ_1 and θ_2 are the two angles of the magnetic moment of the domain with respect to current density, and V_D and V_s are the volumes of the domain and the sample, respectively. If p is the probability of being in one of the two orientations, the variance in R due to the orientation fluctuations is then $\langle(\delta R)^2\rangle = p(1-p)(\Delta R)^2$. Although other magnetic effects can cause resistance noise, we will discuss later why they are not important here.

When individual switching events are not easily resolved, we can deduce the approximate domain size from features in plots of power spectral density vs frequency. The spectral density of fluctuations in R , $S(f, T)$, is described by a conventional parameter α , normalized to be independent of sample size and current;¹⁵

$$\alpha(f, T) \equiv \frac{fS(f, T)N_s}{R^2}, \quad (2)$$

where N_s is the number of atoms in the sample, f is frequency, and T is temperature. The contribution to the total fractional resistance fluctuations of a single two-state fluctuator is then¹⁵

$$\frac{N_s \langle(\delta R)^2\rangle}{R^2} = N_s \left[\frac{\Delta R}{R} \right]^2 p(1-p) = \int_0^\infty \frac{\Delta\alpha(f)df}{f}, \quad (3)$$

where $\Delta\alpha$ is the contribution to α made by the fluctuator being considered.

If we assume that each contribution to $S(f)$ is a Lorentzian,¹⁵ the integral in Eq. (3) simplifies to $\pi\Delta\alpha_{\max}$ ($\Delta\alpha_{\max}$ is the peak in $\Delta\alpha$). For a given V_D the largest possible $\Delta\alpha(f)$ is then found when $p=0.5$ and $(\cos^2\theta_1 - \cos^2\theta_2)=1$. From Eqs. (1) and (3), we then have

$$V_D \geq 2V_s \sqrt{\pi\Delta\alpha_{\max}/N_s} \left[\frac{\Delta\rho}{\rho} \right]^{-1}. \quad (4)$$

Even when individual Lorentzians cannot be resolved in the spectrum, an average domain volume can still be estimated if the spectral slope varies significantly from a constant, i.e., bumps are present in the spectrum. We define v to be the fractional variance of $\alpha(f)$ from a function of constant spectral slope, which serves as a reasonable approximation to an ensemble average of $\alpha(f)$. The essential idea is that v is inversely proportional to the density of individual contributing fluctuators, so that the typical size of the individual fluctuators may still be separated from their density. (Detailed calculations for estimating the domain volumes are given in the Appendix.) After making reasonable (and not critical) assumptions, which are discussed in the Appendix, about a distribution of domain rotation angles ($\theta_1 - \theta_2$), we estimate a minimum typical domain volume (V_{DT} , see Appendix) to be

$$V_{DT} \geq 8V_s \sqrt{v\alpha_{av}/N_s} \left[\frac{\Delta\rho}{\rho} \right]^{-1}. \quad (5)$$

where α_{av} is the average of $\alpha(f)$ over the frequency range of the measurement.

A switching domain's magnetic moment, μ_D , can be approximately determined by measuring the magnetic field H_s that is necessary to eliminate the noise caused by the fluctuator. μ_D may be very crudely estimated from a simple argument: The duty cycle (fraction of the time spent in one of the two levels) and rates of the domain switching events should depend on fields which are large enough for the magnetic energies to be comparable to $k_B T$. Very roughly, $H_s \mu_D \approx k_B T$, where k_B is Boltzmann's constant. Then, for simple ferromagnetic domains, a rough estimate of V_{DT} can be determined from measured quantities to be

$$V_{DT} \approx \frac{\mu_D V_s}{\mu_a N_s}, \quad (6)$$

where μ_a is the magnetic moment per atom, which is on the order of μ_B ,⁷ and can be estimated from Arrott plots⁷

of our magnetization data.

The domains can also reorient due to effects on the free energy which are quadratic in H . The field scale for such effects is essentially the same as the scale for magnetoresistive anisotropy. This scale is about 200 Oe (from 77–300 K) in these films.

EXPERIMENTAL TECHNIQUES

Films were prepared by dual electron-beam deposition at 7×10^{-8} Torr. Two separate depositions were made, denoted by the sample number. In each deposition, several substrates were used simultaneously. Sapphire substrates were used for samples destined for electrical measurements, and a glass cover slide was used for samples analyzed by superconducting quantum interference device (SQUID) magnetometry and the inductively coupled argon plasma (ICP) technique. The films used for magnetometry and chemical analysis are denoted with the subscripts m and c , respectively. In addition, a large sample on glass ($1'_c$) was evaporated immediately after sample 1, with the same deposition rate readings on the crystal monitors.

Sample 1 was about 110 nm thick. ICP gave $x = 0.28$ for sample 1_c and $x = 0.27$ for sample $1'_c$; the two concentrations agree to within the uncertainty of ± 0.01 . Sample 2 was 73 nm thick. ICP gave $x = 0.27$ for sample 2_c .

We used standard photolithography to pattern samples into nearly balanced four-segment bridges, with all four segments parallel. Such patterns give voltages insensitive to fluctuations in T and in probe current.¹⁶ In sample 1 each segment was about $3 \mu\text{m}$ wide by $650 \mu\text{m}$ long. Segments of sample 2 were $6 \mu\text{m}$ wide. An extra segment orthogonal to the others was included for measuring anisotropic magnetoresistance (AMR).

Due to the sensitivity of the magnetic behavior to small metallurgical changes,¹⁴ samples from a single deposition on different substrates (e.g., samples 1 and 1_m) might show slight differences. The AMR measurements, on the other hand, were made on the *same* samples as the noise.

The AMR was measured by comparing the field-induced resistive imbalance of a bridge with one arm parallel to the applied field and the other perpendicular. One measurement was made by applying a field at a series of temperatures cooling between measurements in zero field, and another by subtracting the resistance in a zero-field-cooled (ZFC) run from that in a field-cooled (FC) run. The field used was 3.1 kOe, supplied by a conventional electromagnet. All fields were applied parallel to the bridge segments, so that demagnetizing effects were small.

As a sensitive probe of the onset of slow magnetic dynamics, we measured the out-of-phase response $R''(f_H, T)$ of the AMR to a magnetic field of the form $H(t) = H_0 + H_1 \cos(2\pi f_H t)$, with $H_0 = 288$ Oe, $H_1 = 110$ Oe, and $f_H = 1.56$ Hz.

Noise measurements were made both with simple dc techniques and with conventional ac lock-in techniques, using a probe current at a frequency of 2.33 kHz. We periodically checked for the presence of contact noise by

using various combinations of leads for voltage measurement and for current.

SAMPLE CHARACTERIZATION

Some conventional magnetic characterization is obviously required to constrain the interpretation of the noise data as well as to connect our measurements with others on similar materials. Because the unmanganese concentration was unusually high ($x \approx 0.27$) for ferromagnetism to be present, we believe that these films had some short-range chemical order.¹⁴ In comparing our data with other data on films, one should remember that, as we shall see, the temperature of the onset of high susceptibility cannot be used to infer x .

Because of the complications involved in determining the magnetic ordering of our samples, particular care was taken to demonstrate that these samples exhibited true long-range ferromagnetism and were not simply superparamagnetic with low-temperature cluster glass effects present.¹² SEM images, discussed in the next section, give strong evidence of ferromagnetism in most of the sample. In this section we shall present some magnetization data, as well as static and dynamic measurements of magnetoresistance.

In sample 1_m SQUID magnetometry showed weak differences between the FC and ZFC conditions down to 160 K, below which there was a fairly sharp onset of large remanence (see Fig. 2). Such remanence is expected below the reentrant temperature. Unlike in most bulk data, the films' demagnetizing factor is small, since they were oriented parallel to the field. However, some data on thin samples of rapidly quenched bulk material have been obtained.² These show no remanence for T greater than the ZFC peak of M . Our films are therefore different magnetically from such bulk material.

In sample 1_m the temperature of the onset of ferromagneticlike susceptibility, which we loosely denote as T_c , appeared to be well above the upper limit of this measurement, 300 K. Thus the qualitative magnetic response

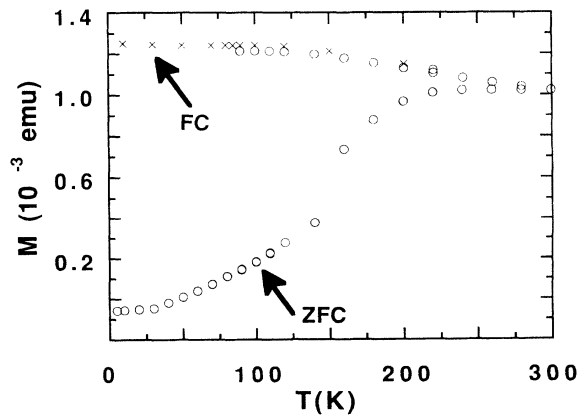


FIG. 2. The magnetization vs T , ZFC (field warmed) and FC in sample 1_m , which had a mass of 4×10^{-4} g. The measuring field was 30 Oe. The two symbols are for data taken at two different times. Large remanence set in at about 160 K.

of this film resembled that of a slowly quenched bulk sample, for which the range of the ferromagnetic order is an open question.¹² Other data on films⁸ also deviate significantly from the phase diagram¹¹ of Fig. 1.

Hysteresis curves provide clear evidence for the presence of highly organized clusters of ferromagnetic domains with 180° domain walls. In sample 1_m there were pronounced waists in the ZFC hysteresis, but these waists were not quite as clean as in the best bulk samples. (See Fig. 3.) Unlike in bulk, some of this unusual character of the hysteresis persisted all the way up to 350 K. At this temperature, magnetization saturated at ~ 500 Oe, a field too low for a superparamagnet, in fact setting a minimum ferromagnetic cluster moment of $\sim 10^4 \mu_B$. The waisted hysteresis loop at 350 K seems to be consistent with the 180° domain walls appearing in both fer-

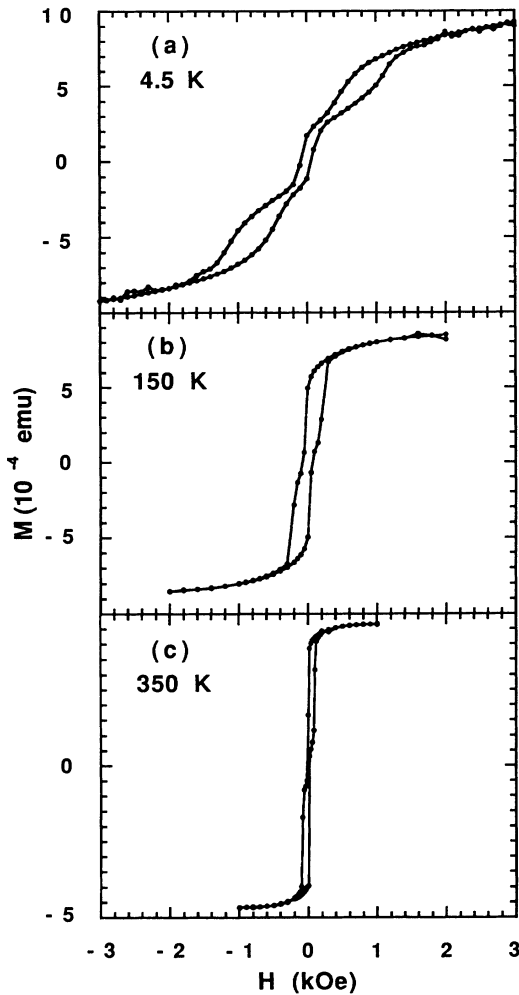


FIG. 3. Magnetic hysteresis. The sample was an 8×10^{-5} g portion of sample 1_m ; (the remainder was used to double check the ICP result). The wasp-waisted hysteresis loop characteristic of disordered NiMn was present at all temperatures but was most pronounced at low temperatures. At 350 K, M almost completely saturated in 1 kOe, showing that the sample was ferromagnetic rather than superparamagnetic. At 4.5 K, on the other hand, M was nowhere near saturation even at 3 kOe, which is more characteristic of a spin glass.

romagnetic and reentrant spin-glass regimes, as seen previously in films by transmission Lorentz microscopy.¹

In sample 1 the two types of AMR curves were essentially identical down to 130 K. At 130 K the ZFC-FC anisotropy leveled off and the anisotropy produced by a field applied at the measuring T decreased [see Fig. 4(a)]. This onset of remanence in the AMR provides a good measure of an apparent reentrant temperature for the actual sample used for noise measurements. The out-of-phase response of the ac AMR, shown in Fig. 4(b), with a small measurement field similar to that in the SQUID measurement, starts to decrease around 180 K. The AMR in the range 200–350 K can be fit with a function which is linear in T , extrapolating to zero at 420 K. At 420 K, a decreasing tail of the AMR is still present, suggesting that a small fraction of the sample has higher T_c . Although substantial AMR would not be present in the simple spin-glass phase or the paramagnetic phase, the presence of AMR does not tell much about the range of any ferromagnetic order.

ZFC magnetization for sample 2_m , shown in Fig. 5, falls off suddenly below 60–70 K. There is an onset of a high-susceptibility regime near 170 K, below which some remanence is found. From 170 to 300 K, there is a small residual magnetization at very low fields, as seen in the nonlinear portion of magnetization in Fig. 5. The difference between $M(20 \text{ Oe})$ and $2M(10 \text{ Oe})$ is virtually independent of T (as shown in Fig. 5) above 220 K, indicating that a small fraction of the sample formed a high-

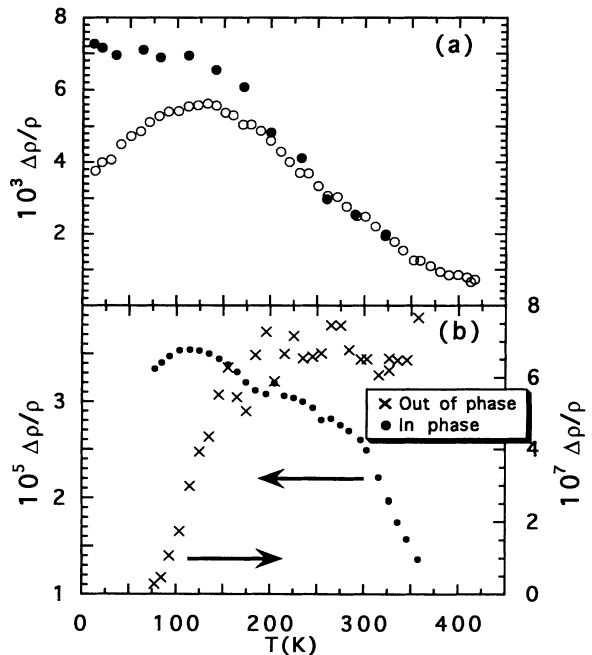


FIG. 4. (a) Anisotropic magnetoresistance, ZFC and FC, of sample 1, which was also used for noise measurements. The AMR approached zero with increasing T , giving an apparent T_c for most of the sample to be about 420 K. Irreversibilities set in below 120 K in this 3.1 kOe field. (b) Real and imaginary (out-of-phase) parts of the response of the AMR to an ac applied magnetic field. The out-of-phase part markedly changed as T decreased below ~ 180 K.

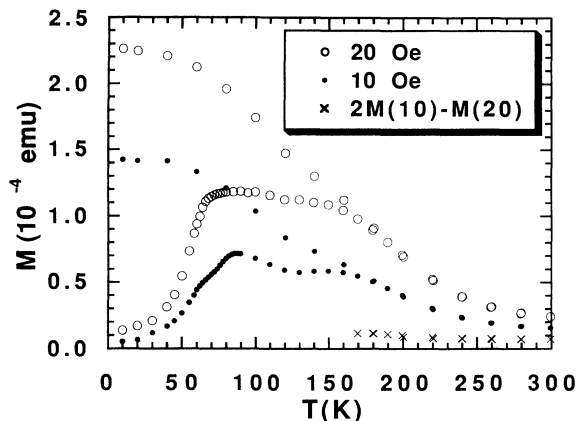


FIG. 5. Magnetization vs T in two different fields for sample 2_m , which had a mass of 4×10^{-5} g. From these data it appears that most of the sample became ferromagnetic below 270 K. The \times symbols show the nonlinear portion of the magnetization, $2M(10 \text{ Oe}) - M(20 \text{ Oe})$, from which the fraction of Ni_3Mn in the sample was estimated. Here, T_{FSG} , taken to be the onset of significant remanence in M (the knee in the ZFC curves), was between 60 and 70 K.

temperature ferromagnet—presumably Ni_3Mn .¹⁷ From the magnitude of this residual magnetization, together with the known magnetization of Ni_3Mn ,¹⁷ we estimate that 0.17% of the material precipitated as Ni_3Mn . Some AMR also persists in sample 2 even above 350 K, consistent with this conclusion.

In sample 1 the high-temperature tail of the AMR was slightly smaller than in sample 2, so that sample 1 presumably had slightly less Ni_3Mn precipitate. Since 0.17% is far below any two-dimensional (2D) percolation threshold, the small amount of high- T_c precipitate in these films cannot account directly for any long-range coherent effects, such as those to be described in the electrical noise.

Hysteresis in the sample 2_m magnetization (Fig. 6) shows a bit of the waist typical of reentrant $\text{Ni}_{1-x}\text{Mn}_x$ curves at low temperatures. However, the effect is much less dramatic than in sample 1.

The overall magnetic behavior is rather complex. The transition temperatures did not correspond well with those of rapidly quenched bulk samples.^{11,12} Sample 1, which has a very high concentration ($x = 0.28$ from the ICP measurement), still has ferromagneticlike susceptibility and AMR up to 420 K, even though the critical concentration for the onset of ferromagnetism in rapidly quenched bulk is $x = 0.24$.⁶ In fact, in sample 1, for T_c this high, no reentrance would be expected for a fully disordered bulk sample. The most likely interpretation is that some short-range chemical order is present, as in slowly quenched or annealed bulk samples showing similar behavior.^{12,14} In addition there is evidence for a small amount of material with very high T_c —probably Ni_3Mn precipitate. As in slowly quenched bulk samples, there is no sharp ferromagnetic transition. In what follows, we shall denote the temperature at which the large remanence appears in the magnetization and the AMR as T_{FSG} , without meaning to imply that this temperature

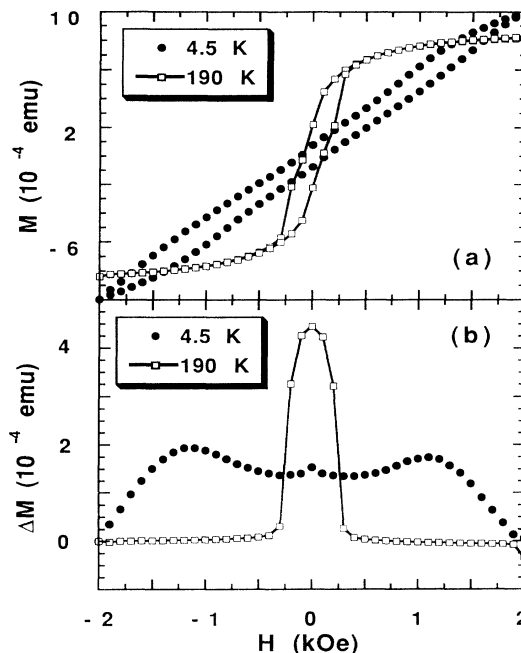


FIG. 6. Magnetic hysteresis of sample 2_m . (a) At 4.5 K the wasp-waisted loop feature of the reentrant spin glass was present, but it was not nearly as dramatic as in sample 1_m . For T above the reentrant regime the loop was typical of ferromagnetic hysteresis. (b) The width of the hysteresis curves is plotted so that the slightly bimodal reentrant behavior at 4.5 K is clearly visible.

represents a sharp phase boundary or that the low-temperature regime closely resembles a standard spin glass.

Considering the hysteresis loop, at least part of each film appears to be ordered in the way that the model of Kouvel and Abdul-Razzaq³ describes, with clusters of antiferromagnetically aligned ferromagnetic domains. Whether such domain clusters act as dynamically coherent units will be revealed by the noise measurements.

SEM

Sample 1_m was imaged at room temperature at 20 kV with a Hitachi S-800 SEM which had a field emission tip. As seen in Fig. 7, even at room temperature there are small, systematic ripples in the contrast of the image, characteristic of ferromagnetic domain images. These ripples appear to come from domains with mainly 180° domain walls. The domains tend to be fairly close to straight lines; their curvature in the photograph is somewhat exaggerated because 30° tilting of the sample without compensation causes surface roughness to account for some of the curvature. Several micrographs were taken, and Fig. 7 is only a part of one with relatively good contrast in the domain structure. Contrast between alternate domains tended to be visible where the film was fairly flat, although some domains were seen to pass through small bumps and ridges on the surface without being significantly affected. The average width of domains in different regions was rather constant,

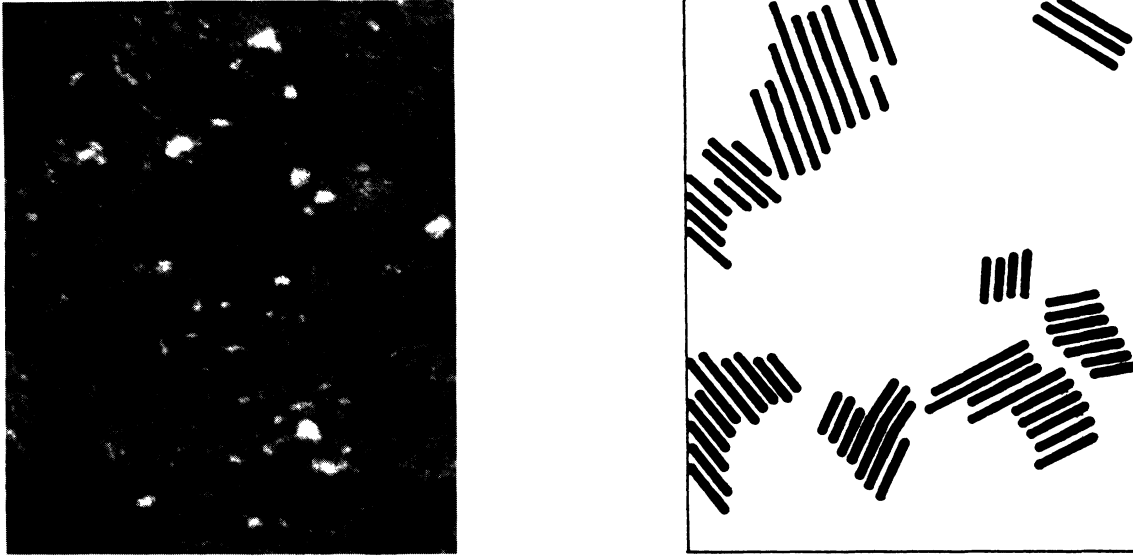


FIG. 7. A room-temperature SEM image of a piece of sample 1_m . The full view of this photograph is $0.48 \mu\text{m}$ by $0.38 \mu\text{m}$. The sketch next to the photograph shows stripes corresponding to the places in the photograph where domains can be seen. Other images also were obtained (discussed in the text).

(6.7 ± 0.2) nm, but contrast was too faint over most of the image to determine how systematic the antiferromagnetic arrangement of domains was.

Contrast was strongest for domains oriented parallel to the tilt axis (vertical in Fig. 7), and no domains were visible which were almost perpendicular to the tilt axis. This highlighting of domains preferentially according to their orientation is what is expected for the "type II" contrast mechanism,¹⁸ in which electrons are steered toward or away from the film surface by a magnetic field parallel to the tilt axis, and thus are backscattered more or less than electrons in zero magnetic field would be.

Since some domains are bound to be aligned nearly perpendicular to the tilt axis, and thus would give insufficient contrast, and since surface features obscured domains over part of the sample, we can only estimate a lower bound of the coverage of ferromagnetic domains over the sample. At least half of the film was ferromagnetically ordered. Although the SEM images do not tell us the order of the remaining material, the natural interpretation is that it is also predominantly ferromagnetic.

Clearly, in spite of short-range chemical order, these samples have long-range magnetic order at high temperatures. We now turn to the noise to study the domain dynamics.

NOISE RESULTS

The dependence on T of the noise magnitude parameter α of sample 1 above 70 K is plotted in Fig. 8. The most prominent result is a peak between 100 and 150 K. Typical spectra are shown in Fig. 9, exhibiting large spectral features of this high-temperature noise. Such features are far too large to be consistent with ordinary

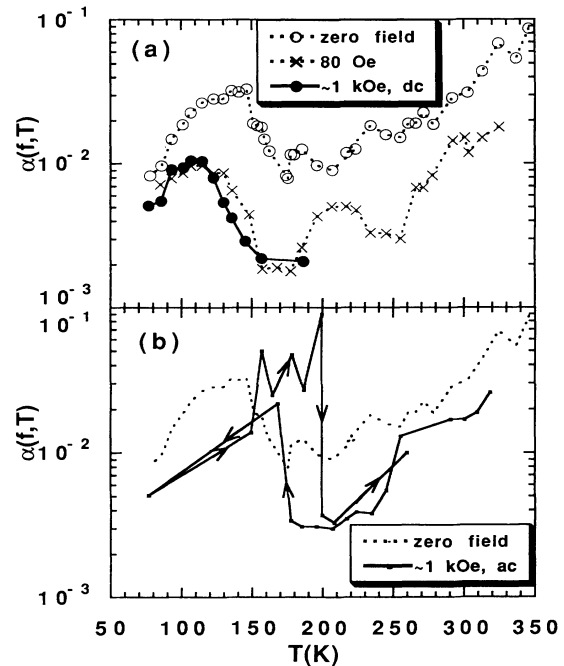


FIG. 8. α vs T in the ferromagnetic regime of sample 1. (a) α vs T in zero field, 80 Oe, and ~ 1 kOe. The 1-kOe data used a dc probing current, and erratic ac-field-driven data in $H=0$ and 80 Oe have been omitted for clarity. Ferromagnetic noise was almost completely suppressed in the field. (b) α vs T at ~ 1 kOe measured with an ac probing current. Some domain fluctuations were excited by the ac field. The transition exhibited hysteresis, seen by following the arrows, which track the data in the order in which it was taken. The zero-field α vs T data are plotted as a dotted line for comparison.

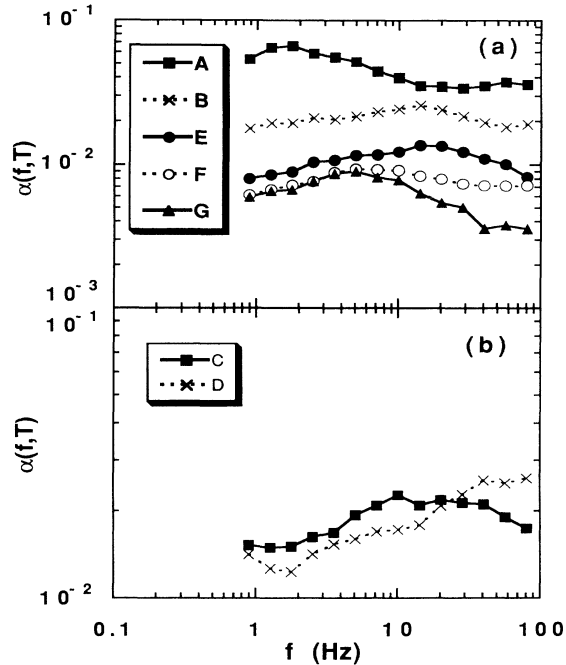


FIG. 9. Sample 1, α vs f in the ferromagnetic regime, highlighting spectral features. (a) A and B are ac-current (field)-induced noise at 170.6 K and 173.3 K, showing the large features and increased noise. E , F , and G are noise that appeared when the sample was cooled in a field. E has $T=259.8$ K and $H=1$ kOe, F has 93.0 K and 80 Oe, and G has 207.2 K and 44 Oe. Although noise was significantly suppressed, neither noise nor features were eliminated even in 1 kOe field, presumably because different domains were free to fluctuate than those seen at other fields. (b) C and D are spectra with features seen in zero field at 260.8 and 234.3 K.

noise from defects in metals, but features arising from magnetic effects have been found in smaller samples of several other magnetic metals.^{19,20}

The noise in the ferromagnetic regime of sample 1 was, on the average, suppressed in small magnetic fields. Figure 8 illustrates the noise suppression in a 1 kOe field. 80 Oe was sufficient to suppress most fluctuations above 100 K except for one peak in α near 215 K and another broad peak which was not very sensitive to field effects at about 115 K.

These two peaks in α were easily resolved above the background of noise from smaller domains. Their frequency-temperature dependences could be well fit with an Arrhenius expression, $f = f_0 e^{E_a/kT}$, yielding activation energies E_a and attempt rates f_0 . The peak at 115 K (the only remaining large fluctuator when a 1-kOe field was applied) had an activation energy of 0.17 eV and attempt rate of approximately 10^9 Hz. The other peak, seen in an 80-Oe field, had an activation energy of 0.49 eV and an attempt rate around 5×10^{12} Hz. Discrete switching events were barely resolvable above the other noise in the time domain.

Below about 100 K in Sample 1, $\alpha(f, T)$ grew as T decreased, but with extreme variability between different cooldowns. Nearly every time the sample was cooled

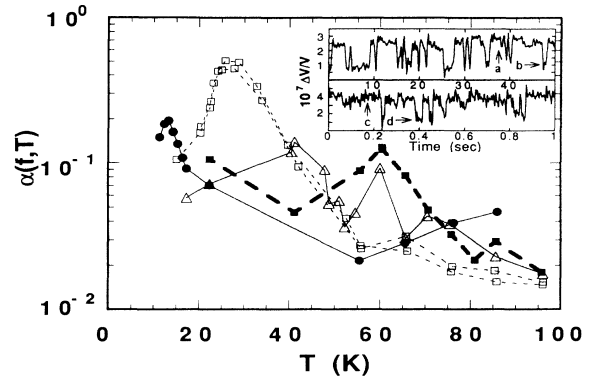


FIG. 10. Sample 1, α vs T at 3 Hz for several successive cool-downs in the reentrant regime. Different peaks correspond to different fluctuating clusters of domains which happened to appear in this frequency window. Inset: Switchers in the time domain. In the upper box the step size is $\Delta R/R = 1.8 \times 10^{-7}$. The two distinct states are labeled a and b . Data were taken at 70 K. The upper box is a time series of the switcher with its spectra shown in Fig. 11, and the lower box plots the switcher of Figs. 12 and 13. In the lower box $\Delta R/R = 2.4 \times 10^{-7}$, and $T = 50$ K. The two states are labeled c and d . $\Delta R/R$ gives $V_D \geq 3 \times 10^{-14}$ cm³ (discussed in the text).

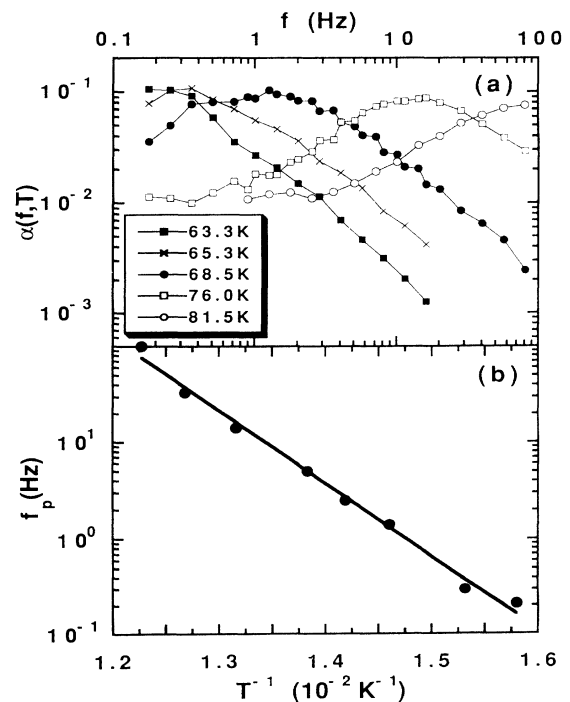


FIG. 11. (a) α vs f of sample 1 at several indicated temperatures is shown in a regime dominated by one switcher. The power spectral density was nearly a Lorentzian in f , as is expected for individual switchers (Ref. 15). (b) An Arrhenius plot of the frequency of the peak in α vs $1/T$. The straight line is a least-squares fit to the Arrhenius law, giving an activation energy of 136 meV and an attempt rate of 6×10^{10} Hz.

from above 200 K, one or two large, distinct two-state switchers, such as those shown in the inset of Fig. 10, dominated the noise in this regime. Fig. 10 shows $\alpha(f, T)$ vs T for several cool-downs, together with noise in the time domain corresponding to two different peaks in $\alpha(f, T)$ vs T . The step sizes shown, $\Delta R/R \approx 2 \times 10^{-7}$, were typical. These switchers' characteristic rates also showed strong Arrhenius temperature dependences, as seen in Fig. 11.

Field changes as small as 0.04 Oe caused noticeable changes (partly transient) in the characteristic rates associated with a switcher, confirming that these are in fact magnetic domains of some sort, not some huge fluctuating structural defects. Figure 12 illustrates such effects. However, typical switchers remained active over field ranges in excess of 300 Oe. Figure 13 shows that the step size of one typical fluctuator remained nearly constant with changes of field of 125 Oe. This range is roughly

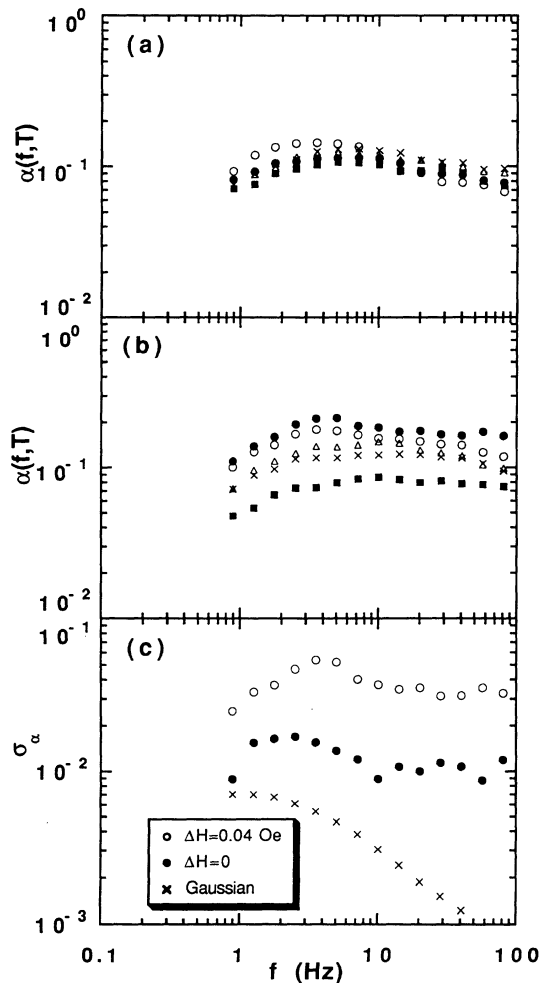


FIG. 12. (a) Five measurements of α vs f before the magnetic field was changed by 0.04 Oe. The peak frequency was relatively constant. $T = 50$ K. (b) α vs f after the small field change. (c) The standard deviation of the five measurements of $\alpha(f, T)$ vs the frequency. The lowest curve is the expected standard deviation for Gaussian noise. It is clear that the slight change in field produced significant transient effects on the noise spectrum.

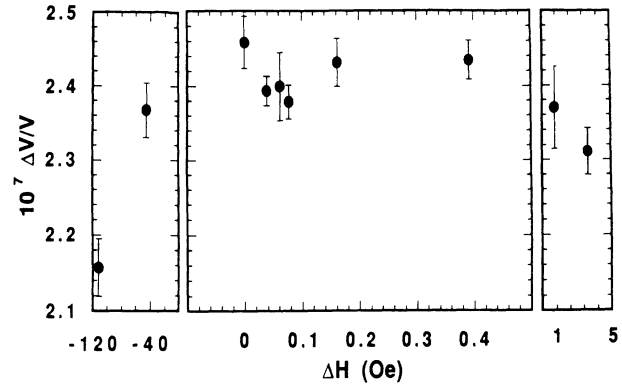


FIG. 13. Step sizes vs H of the switcher with spectra plotted in Fig. 12. Horizontal lines were drawn to match the lower and upper voltage states on plots similar to the lower inset of Fig. 10, and the step size was taken to be the distance between the lines in units of $\Delta V/V$. Each point here came from averaging sizes of ~ 100 switching events, and error bars are the standard deviation of the mean of these event sizes, where the scatter is due to other noise sources. These data clearly show that the same fluctuating object was observed over a field range of at least 120 Oe. Step sizes on other cool-downs were similarly independent of H .

consistent with the field scale for domain reorientation obtained from AMR.

α vs T of sample 2 is plotted in Fig. 14. The spectral features were less prominent than in sample 1. Overall, the noise magnitude was suppressed only in fields of at least a few kOe. These results point toward smaller fluctuating regions with smaller net magnetic moments than in sample 1. The low-temperature giant switching noise of sample 1 did not show up in sample 2.

In sample 2, the noise measurements extend to temperatures well above those for which most of the sample is ferromagnetic. The noise is still strongly suppressed in moderate fields, but does not show the spectral features found at lower temperatures.

Although individual peaks in spectra of sample 2 were not easily distinguishable, weaker features appeared in

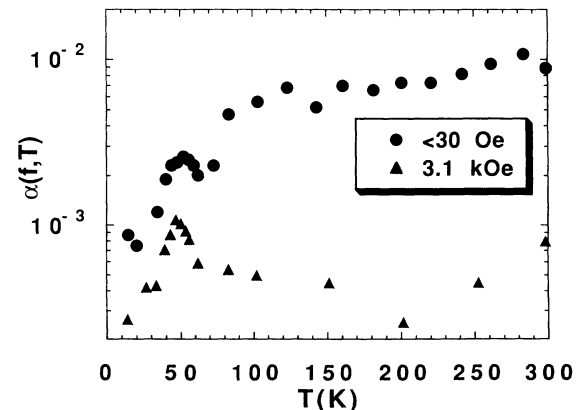


FIG. 14. Sample 2, α vs T . This sample, while not exhibiting large switching noise in the FSG state, showed ferromagnetic noise diminishing at low T , as well as a noise peak at about 47 K which was not suppressed in fields up to 3 kOe.

most spectra taken below 200 K. These features can be quantitatively described by the variance in α , v , defined in the "background" section. Using spectra from nine different temperatures in the range 70–190 K, we found an average $v \approx 0.004$. Above 190 K no statistically significant features were found in $\alpha(f)$.

We expected to find some noise from spin-glass dynamics coupled to R via universal conductance fluctuations (UCF's), as found in CuMn ,²¹ AuFe ,²² and the reentrant $\alpha\text{-FeZr}$.²⁰ Such noise would be Gaussian and featureless in samples as large as those described here. Sample 2 showed a peak in α vs T around 47 K, a little below the T_{FSG} determined from the SQUID data. This peak, which was not suppressed in fields up to 3 kOe, clearly has a different origin than the domain noise, and might be related to the onset of spin-glass order. A systematic study of this noise was not easy, due to the large ferromagnetic domain noise. No distinct spectral features were resolved in the narrow regime in which this peak dominated the noise.

An unidentified first-order transition, with thermal hysteresis, was found near 190 K in the resistance and the noise of sample 1. The noise measurements made with an ac probing current were much larger in the temperature range near 190 K than identical measurements made with a dc probing current. Apparently, the 2.33-kHz ac fields of ~ 1 Oe produced by the measuring current were sufficient in this temperature range to excite some domain motion; this effect was found in some other ferromagnetic films.²⁰ As seen in Fig. 8(b), the noise probed by ac current rose erratically by about an order of magnitude at 170 K and subsided at lower temperatures, and at 200 K during warming α dropped suddenly by a factor of 3 to approximately the dc-probed value and remained there at higher temperatures. At the same time the resistance jumped by more than 5 parts per 10^6 . The larger ac-probed noise also contained much larger features in its spectra than the dc data (see Fig. 9). Discontinuities in the resistance vs temperature curves appeared in sample 1 and also in another sample grown and fabricated together with it. Some large spectral features appeared and then disappeared when field was varied by ~ 30 Oe at 188 K. We suspect that the film anisotropy played a role in these phenomena, but do not have sufficient evidence to warrant discussing them further in this paper.

CONCLUSIONS

Since most of the noise found in the ferromagnetic regime is suppressed in a rather small field, it must come from some magnetic source. The presence of identifiable features is highly unusual for metallic samples of this large size,¹⁵ again indicating an origin in the dynamics of large domains.

If the domain dynamics cause noise simply because of the SRA, we may calculate the domain size via Eq. (4). (The SRA is approximately the AMR at these temperatures.) For sample 1 we find $V_D \approx 4 \times 10^{-15} \text{ cm}^3$ in the ferromagnetic regime—a somewhat surprising result since the domains visible in the SEM images are not that large. However, since $H_s \approx 80$ Oe, $\mu_D \approx 10^5 \mu_B$, a much

smaller moment than would be found for a ferromagnetic domain of volume $4 \times 10^{-15} \text{ cm}^3$. For the two large individually resolved fluctuators, we had $V_D \approx 2 \times 10^{-14} \text{ cm}^3$, and the apparent moment was even smaller than for typical domains.

In order to have a low net moment even though the net volume is large, domains must rotate in clusters which consist of ferromagnetic domains with 180° domain walls. The moments of adjacent ferromagnetic domains cancel but their SRA adds.

Very similar results were obtained for the ferromagnetic regime of sample 2 below 200 K. Since independent peaks in its spectra were not easily distinguishable, we used Eq. (5) to estimate V_{DT} . The SRA was $\sim 5 \times 10^{-3}$, and $v \approx 0.004$. Then, from Eq. (5) $V_{\text{DT}} \geq 9 \times 10^{-16} \text{ cm}^3$.

At this point we should consider alternatives to the hypothesis that the SRA is the dominant mechanism by which the magnetic fluctuations couple to the resistance. If there were some larger term by which magnetic noise affected R , then Eqs. (4) and (5) would overestimate V_D , perhaps leading to a qualitatively incorrect picture of the domain clusters.

Magnetoresistive noise effects at domain boundaries²³ would be too small to cause the observed noise unless the fluctuating domains were at least $0.9 \mu\text{m}$ in perimeter (in sample 1); this assumes only that the magnetoresistive effects are no more than 100% of the resistance within one mean free path of the boundary. We cannot presently rule out the possibility that domain boundary magnetoresistive effects contribute to the noise, but allowing for them cannot significantly reduce the estimate of the domain size.

Other mechanisms which couple magnetism to resistance, which do not invoke ferromagnetic domains, would be insufficient to account for such large individual fluctuations in the resistance. For UCF coupling of locally random spin arrangements to R ,²⁴ for example, such large fluctuations would require the rearrangement of more than about 100% of the spins in the entire sample.

The field-dependent noise in sample 2 above 270 K must come from the tiny fraction of the sample which is ferromagnetic. The absence of spectral features above 190 K means that we cannot set a minimum domain size from the noise. The obvious interpretation is that all the field-dependent noise above 270 K and part of the noise at lower temperatures is due to numerous small, uncoupled ferromagnetic domains—just as expected for Ni_3Mn precipitates. These cannot, however, account for the large coherent fluctuators found only at temperatures below 190 K, well into the ferromagnetic regime.

The large switching noise found at low temperatures in sample 1 is the most striking and unusual feature of our results. The resistance steps found for $T < T_{\text{FSG}}$ were about seven times larger than those inferred from the noise features at higher T . For such large steps, explanations other than SRA of rotating domains become even more unrealistic than for the noise features in the ferromagnetic regime.

The field scale for the suppression of these low-temperature fluctuators was slightly larger than that of the ferromagnetic noise, being several hundred Oe for the

fluctuator shown in Figs. 10, 12, and 13. That field scale implies a total moment of roughly $10^3 \mu_B$. Nevertheless, the existence of observable effects on the switching for fields as small as 0.04 Oe indicates that there are some degrees of freedom associated with these domains which have moments roughly on the order of $10^7 \mu_B$.

The evidence thus suggests very strongly that these large low-temperature fluctuators are also clusters of ferromagnetic domains which align antiferromagnetically over a long range. Ordering into 180° domain-wall patterns in the ferromagnetic regime is consistent with the high-temperature hysteresis loops, our SEM images, and others' TEM observations of films¹ that showed similar ordering in the reentrant and ferromagnetic regimes. The volume of the clusters which rotate coherently is about $3 \times 10^{-14} \text{ cm}^3$, calculated from $\Delta R/R$ and Eq. (1), corresponding to an area of $0.3 \mu\text{m}^2$.

The lack of the giant low-temperature switching noise in sample 2 points to less long-range antiferromagnetic clustering than found in sample 1. Such an interpretation is strongly supported by the relatively subtly bimodal exchange field inferred from the hysteresis loop of sample 2_m, as compared with sample 1_m. Since the characteristic T_c and T_{FSG} also differ between the two samples, they presumably differ in their short-range atomic order. At any rate, the evidence from noise agrees with that from the magnetic hysteresis.

One clear result of our measurements is that the films show extensive ferromagnetic order. These films, like bulk samples with some short-range order, had a regime of high ZFC susceptibility which extended over a greater temperature range than found in completely disordered solid solutions. Thus it is possible that such bulk samples with partial short-range order also have extensive ferromagnetic order, despite their lack of clear critical behavior. It is interesting that in reentrant Fe_xZr_{1-x} films experimenters have also detected extensive domains that have not been observed in bulk samples.^{20,26}

From the SEM images, static cluster sizes seem to be limited at least partly by film inhomogeneities and defects. The cluster sizes could vary significantly with film growth quality.

The fluctuating clusters have a systematic net antiferromagnetic alignment of their constituent ferromagnetic domains. In the ferromagnetic regime of sample 1 the constituent moments of the domains in a typical coherent cluster canceled each other to about 1 part in 500. In the reentrant regime the constituent magnetic moments canceled to about 4 parts in 10^6 . In sample 2 cancellation was to about 1 part in 10^5 at 80 K.

The resistance noise measurements led directly to a domain-cluster model identical to that proposed on less direct evidence by Kouvel and Abdul-Razzaq. We should point out that noise results led us to this domain model despite our lack of awareness of its prior existence—which demonstrates (in addition to our prior ignorance) both the power of the noise techniques and the genuine predictive value of the model.

The noise measurements show that clusters qualitatively similar to those found in the reentrant regime are already present in the ferromagnetic regime, at least in these films. The cluster coherence volume, however, is generally larger in the reentrant regime.

ACKNOWLEDGMENTS

Primary support came from NSF Grant No. DMR 89-22967. Extensive use was made of Materials Research Lab facilities and of fabrication apparatus of R. S. Averback, funded by NSF Grant No. DMR 89-20538. We thank Vania Petrova for help getting the high-resolution SEM images, and Lilian Hoines and Rick Michel for stimulating discussions.

APPENDIX

We use the line of reasoning found in Ref. 25 to obtain an estimate of domain volume from α and its fractional variance, v_e , about its ensemble average. n' is the number of individual Lorentzian contributions to the fluctuations per factor of e in characteristic rate and per factor of e in $p/(1-p)$. For a fixed domain volume, n' is proportional to α_{av} but inversely proportional to v_e , allowing n' and the typical domain volume each to be determined. The average α is

$$\alpha_{av} = n' \left[\frac{\Delta\rho}{\rho} \right]^2 \frac{\langle N_d^2 \rangle}{N_s} \langle (\cos^2\theta_1 - \cos^2\theta_2)^2 \rangle.$$

The average $\langle \dots \rangle$ is taken over the collection of fluctuators. Using the results of Ref. 24 we find

$$n' = \frac{1}{3\pi^2 v_e} \frac{\langle (\cos^2\theta_1 - \cos^2\theta_2)^4 \rangle}{\langle (\cos^2\theta_1 - \cos^2\theta_2)^2 \rangle^2} \frac{\langle V_D^4 \rangle}{\langle V_D^2 \rangle^2}.$$

Combining these equations gives

$$\frac{\langle V_D^4 \rangle}{\langle V_D^2 \rangle^2} = 3\pi^2 v_e \frac{V_s^2}{N_s} \frac{\langle (\cos^2\theta_1 - \cos^2\theta_2)^2 \rangle}{\langle (\cos^2\theta_1 - \cos^2\theta_2)^4 \rangle} \left[\frac{\Delta\rho}{\rho} \right]^{-2} \alpha_{av}.$$

Since it is calculable, we take $V_{\text{DT}} \equiv (\langle V_D^4 \rangle / \langle V_D^2 \rangle)^{1/2}$ as the typical domain volume. It's larger than the rms V_D but smaller than the maximum V_D .

We find

$$\frac{\langle (\cos^2\theta_1 - \cos^2\theta_2)^2 \rangle}{\langle (\cos^2\theta_1 - \cos^2\theta_2)^4 \rangle} = \frac{35}{16}$$

for an isotropic distribution of solid angles. Reasonable assumptions about the distribution cannot give much smaller values, but larger values are possible if $|\theta_1 - \theta_2|$ is always small. Thus a reasonable approximation is

$$V_{\text{DT}} \geq 8V_s \left[\frac{\Delta\rho}{\rho} \right]^{-1} \sqrt{v_e \alpha_{av} / N_s}$$

with larger estimates applying if the rotation angles are small.

- ¹S. Senoussi, S. Hadjoudj, and R. Fourmeaux, *Phys. Rev. Lett.* **61**, 1013 (1988).
- ²I. Mirebeau, S. Itoh, S. Mitsuda, T. Watanabe, Y. Endoh, M. Hennion, and P. Calmettes, *Phys. Rev. B* **44**, 5120 (1991).
- ³J. S. Kouvel and W. Abdul-Razzaq, *J. Magn. Magn. Mater.* **53**, 139 (1985); W. Abdul-Razzaq and J. S. Kouvel, *Phys. Rev. B* **35**, 1768 (1974).
- ⁴S. Senoussi, *Phys. Rev. Lett.* **56**, 2314 (1986).
- ⁵S. Senoussi and Y. Oner, *J. Appl. Phys.* **55**, 1472 (1984); *J. Magn. Mater.* **40**, 12 (1983).
- ⁶W. Abdul-Razzaq and J. S. Kouvel, *Phys. Rev. B* **35**, 1764 (1987), and references therein.
- ⁷Hatsuo Tange, Toshihiko Tokunaga, and Mitita Goto, *J. Phys. Soc. Jpn.* **45**, 105 (1978).
- ⁸W. Abdul-Razzaq and M. Wu, *J. Appl. Phys.* **69**, 5078 (1991).
- ⁹H. Kunkel, R. M. Roshko, W. Ruan, and G. Williams, *J. Appl. Phys.* **69**, 5060 (1991); H. Ma, Z. Wang, H. P. Kunkel, Gwyn Williams, and D. H. Ryan, *ibid.* **67**, 5964 (1990).
- ¹⁰K. H. Fischer and J. A. Hertz, *Spin Glasses* (Cambridge University, Cambridge, 1991); K. Binder and A. P. Young, *Rev. Mod. Phys.* **58**, 801 (1986).
- ¹¹R. L. Sommer, J. E. Schmidt, and A. A. Gomes, *J. Magn. Magn. Mater.* **103**, 25 (1992); *J. Appl. Phys.* **73**, 5497 (1993).
- ¹²H. Kunkel, R. M. Roshko, W. Ruan, and G. Williams, *Philos. Mag.* **63**, 1213 (1991).
- ¹³I. A. Campbell, A. Fert, and O. Jaoul, *J. Phys. C Suppl.* **1**, S95 (1970).
- ¹⁴V. I. Goman'kov, A. D. Gyoalyan, B. N. Tret'yakov, K. V. Trush, and V. V. Sumin, *Fiz. Met. Metalloved.* **70**, 49 (1990) [*Phys. Met. Metallogr.* **70**, 45 (1990)].
- ¹⁵M. B. Weissman, *Rev. Mod. Phys.* **60**, 537 (1988).
- ¹⁶G. B. Alers, M. B. Weissman, R. S. Averback, and H. Shyu, *Phys. Rev. B* **40**, 900 (1989).
- ¹⁷S. K. Sidorov and A. V. Doroshenko, *Fiz. Met. Metalloved.* **20**, 44 (1965) [*Phys. Met. Metallogr.* **20**, 40 (1965)].
- ¹⁸D. E. Newbury, D. C. Joy, P. Echlin, C. E. Fiori, and J. I. Goldstein, *Advanced Scanning Electron Microscopy and X-Ray Microanalysis* (Plenum, New York, 1986), Chap. 4.
- ¹⁹N. E. Israeloff, M. B. Weissman, G. A. Garfunkel, and D. J. VanHarlingen, *Phys. Rev. Lett.* **60**, 152 (1988); R. P. Michel, N. E. Israeloff, M. B. Weissman, J. A. Dura, and C. P. Flynn, *Phys. Rev. B* **44**, 7413 (1991).
- ²⁰R. P. Michel and M. B. Weissman, *Phys. Rev. B* **47**, 574 (1993).
- ²¹N. E. Israeloff, M. B. Weissman, G. J. Nieuwenhuys, and J. Kosiorowska, *Phys. Rev. Lett.* **63**, 794 (1989); M. B. Weissman and N. E. Israeloff, *J. Appl. Phys.* **67**, 4884 (1990); N. E. Israeloff, G. B. Alers, and M. B. Weissman, *Phys. Rev. B* **44**, 12 613 (1991); M. B. Weissman, N. E. Israeloff, and G. B. Alers, *J. Magn. Magn. Mater.* **114**, 87 (1992).
- ²²K. A. Meyer and M. B. Weissman (unpublished).
- ²³H. T. Hardner, M. B. Weissman, M. B. Salamon, and S. S. P. Parkin, *Bull. Am. Phys. Soc.* **38**, 619 (1993).
- ²⁴B. L. Al'tshuler and B. Z. Spivak, *Pis'ma Zh. Eksp. Teor. Fiz.* **42**, 363 (1985) [*JETP Lett.* **42**, 447 (1985)]; S. Feng, A. J. Bray, P. A. Lee, and M. A. Moore, *Phys. Rev. B* **36**, 5624 (1987).
- ²⁵G. A. Garfunkel, G. B. Alers, and M. B. Weissman, *Phys. Rev. B* **41**, 4901 (1990).
- ²⁶S. Senoussi, S. Hadjoudj, P. Jouret, J. Billotte, and R. Fourmeaux, *J. Appl. Phys.* **63**, 4080 (1988).

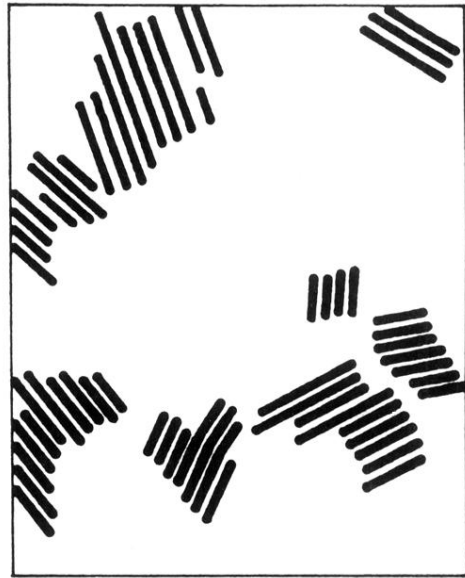
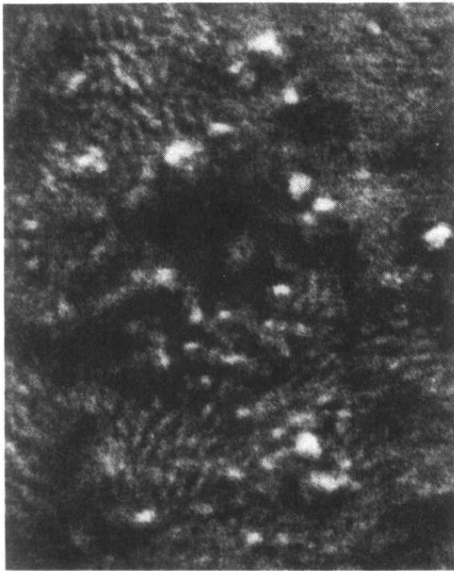


FIG. 7. A room-temperature SEM image of a piece of sample 1_m . The full view of this photograph is $0.48 \mu\text{m}$ by $0.38 \mu\text{m}$. The sketch next to the photograph shows stripes corresponding to the places in the photograph where domains can be seen. Other images also were obtained (discussed in the text).